3D Reconstruction of Reefs using Autonomous Surface Vessels and an Analysis of Chain vs 3D Rugosity Measurement Robustness

Derek Benham, Aaron Newman, Kalai Ellis, Richard Gill, and Joshua G. Mangelson

***Abstract*— Coral reefs are at risk. To study and minimize the impacts of global warming, pollution, or land sediment disposition on the reef, regular and accurate measurements are needed to assess the coral's health. We present a method of using surface vessels to autonomously collect GPS tagged images to be used in creating a 3D model of the reef which we tested in Molokai, Hawaii. We also discuss the shortcomings of chain rugosity measurements (the longtime standard for categorizing reef health) and how surface complexity measurements, a metric only obtained from creating 3D models from imagery are less subject to these flaws.**

I. Introduction

Coral reefs are the most bio-diverse marine ecosystem on the planet. Due to climate change, many reefs are at risk, threatening the entire ecosystem and the humans who depend on them [1][2]. Understanding and measuring the complexity of these ecosystems is essential to counteracting these risks. The current standard for characterizing reef complexity is "chain rugosity". Rugosity is the ratio of the 2D distance the chain travels when laid over the reef to the 1D length of the chain–the greater the value, the higher the complexity. However, this method is invasive, labor intensive, and often suffers from measurement bias. Recent approaches have utilized the photogrammetry technique Structure-from-Motion (SfM) to estimate a simulated linear rugosity [3]. These SfM techniques require image sets with conditions such as large overlap and high resolution. Methods such as autonomous underwater vehicles (AUVs), unmanned arial vehicles (UAVs), and manual image acquisition by divers can each perform this image acquisition with various trade offs.

This paper reports on our method of utilizing an autonomous surface vessel (ASV) to reconstruct sections of the fringing reef in Molokai, Hawaii. Our ASV implementation leverages the strengths of AUV and UAV based systems while minimizing their shortcomings. ASVs, are much cheaper and easier to manage than an underwater vehicle, and can survey deeper reefs with better imagery than an aerial drone. Moreover, because ASVs operate on the water surface they have access to GPS (unavailable to AUVs and divers) and have better battery life than UAVs.

In addition to our survey method, we analyze how small deviations in position/orientation can affect the measured rugosity. We then present a measurement called 3D surface complexity, which is the ratio between the 3D surface area and the 2D plane. This is a measurement that can only be found in SfM, and demonstrates an advantage of SfM over the traditional chain rugosity measurement.

D. Benham, A. Newman, K. Ellis, R. Gill, J. Mangelson, are at Brigham Young University.
{drbenham, an283, kalaiellis, richard_gill, joshua_mangelson}@byu.edu.

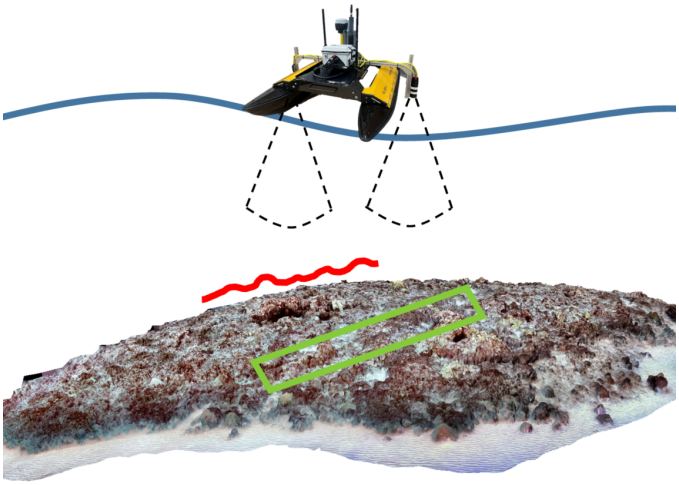

Fig. 1. Conceptual overview of our system that utilizes imagery collected by an autonomous surface vessel to create 3D models of the reef via Structure-from-Motion. To evaluate the reef's health we compare the robustness of the defacto chain rugosity measurements, a 2D/1D metric as shown by the red line, against surface complexity measurements, a 3D/2D metric as shown in green, a measurement that can only be obtained via 3D reconstruction.

II. Related Work

A standard metric for estimating the health of a reef is rugosity, or how complex the reef is. A more complex surface provides more space for smaller coral fish to seek shelter and more surface area for algal symbionts to photosynthesize [4].

Measuring reef rugosity with a chain is a low-cost approach for estimating the health of the reef [5]. A team of divers will wrap a chain over the coral in a linear transect, the shorter the 2D distance the cable travels as it is laid over the coral heads, the higher rugosity value, indicating a healthier, more complex reef. This method has drawbacks because it requires trained divers, measurements may face location bias, only a few measurements can be performed, and measurements may damage the coral.

Regardless of training or safety measures to negate risk, there will always be an inherent safety risk whenever humans enter the water to perform these measurements [6]. Besides the safety concerns, due to the time intensive task of wrapping a chain around coral, only a few measurements can

be obtained. Later, we discuss how additional measurements can be leveraged to infer the true rugosity value.

SfM [7][8], a common photogrammetric technique for estimating 3D structure from a sequence of 2D images, has more recently been applied to solving this issue [3]. SfM is a process that uses overlapping imagery to create robust 3D models. Unique features are extracted from each image and then matched across all images, when a match is found this feature becomes a tie point. Image correspondence is calculated between frames using tie points to create an initial point cloud of the model, then a dense point cloud, and finally a tiled model from the images is overlayed to create a 3D model of what was surveyed. A digital elevation model (DEM) can also be generated for inferring elevation changes across the model as well. This technique however, requires high quality, overlapping images, typically a 70% overlap.

Frequent surveying is needed to effectively monitor change. Current implementations to gather underwater imagery for SfM models require divers [3][9][10], AUVs [11], UAVs [12][13], and even cameras mounted to a body-board [14] for image acquisition. Due to human error, and oxygen requirements, divers can only survey smaller areas to ensure sufficient image overlap. Besides the time requirement and oxygen constraint to survey larger areas, currents can cause even a trained diver to drift off course and miss images that would be needed to ensure successful model reconstruction. Typically, divers use a single camera, usually a GoPro, to capture images; however, a single camera system suffers because scale cannot be inferred. To correctly scale the model, a measurement baseline, a 1m rod, is laid on the ocean floor that will be used in post processing to scale the model accordingly.

AUVs overcome these human errors by producing highly localized images and ensuring overlap. They don't require oxygen and have battery life in the range of several hours. AUVs use accurate pressure sensors to know the vehicle's depth, and will run SLAM (simultaneous localization and mapping) [15] using key features of the seafloor obtained visually with cameras [16] or by acoustics via sonar [17], to estimate vehicle position and pose. Similar to the diver, these vehicles can take highly detailed photos of the reef by traveling as close as a meter above the seafloor. The only downsides to all these benefits is the required complexity to achieve them, which translates to a higher cost and a difficult user interface. Vehicles cost upwards of four hundred thousand dollars and require skilled users to interface with and maintain the machine.

Contrary to AUVs, UAVs present a cheap and easy solution for surveying reefs. An UAV can be flown with minimal training and can be commercially purchased for a few hundred dollars. Casella et al. [13] used UAVs to perform SfM models over shallow reefs, recording an area of 8320 m^2 over the duration of a 10 minute flight. They were however limited to shallow water reefs of less than 1m depth, their flights required calm waters, low wind and minimal sun glint. The end result has the lowest model resolution of all the discussed methods.

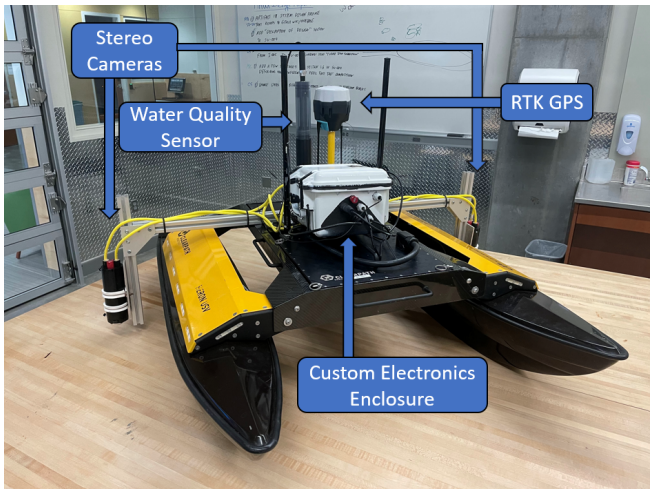

Fig. 2. Labeled survey components on Heron ASV used to obtain reef imagery.

Another method to collect these images is through an ASV. We are not the first research group to utilize an ASV to create bethnic surveys of reefs. Raber and Schill [14] developed a low cost vehicle by outfitting a foam body board with consumer electronics and two Sony a6300 24 Megapixel cameras. Their approach was successful at creating a simple system capable of autonomously traversing a given mission area that ensures sufficient image overlap to create successful 3D reef reconstructions. Due to their objective to create a low budget implementation, their vehicle can only capture images at 0.75Hz, and is unable to GPS tag images. A lack of an image's GPS information significantly increases the computation time for reconstructing images, requiring each image to be compared with every other image rather than solely its local neighbors. In addition to increased computation time, lack of GPS metadata can affect model scaling accuracy as well as only providing relative spatial data.

One thing that should be noted is our use of simulated chain rugosity measurements as opposed to real chain rugosity measurements. Bayley et al. [9] in a comparison survey of the chain method and SfM models concluded that simulated chain rugosity measurements in SfM models are accurate and can be used in lieu of manual measurements. This conclusion is important because it allows us to perform a statistical analysis on our simulated chain measurements as if they were real values collected in the field. Friedman et al. [11] proposed a novel surface area rugosity measurement that projects the area onto a plane using SfM models. Despite proposing a more robust and accurate method, the linear chain method is still used to compare data with historical results. In this work we attempt to quantify the error of these metrics.

III. Autonomous Reef Reconstruction via ASVs

We outfitted an ASV with the necessary sensors to automatically localize and collect the required data. Our approach is a fraction of the cost of an AUV, can take better images

in deeper environments than an UAV, as well as embed GPS data into images unlike the retrofitted bodyboard method.

A. ASV System

Our system was built upon the Heron ASV by Clearpath, see Figure 2. The Heron is a four foot pontoon vessel with a payload compartment and an onboard computer. We chose this platform for its wider beam to help stabilize the boat which allows testing in rougher waters and the use of larger payloads. The larger payload was an interest as it enables future additions of sensors. To achieve a streamlined system we stripped the vehicle of its overhead software apart from a ROS [18] topic that controls the motor output and the subsystem that allows a manual controller override via a generic RC remote.

With the end goal of a vehicle capable of creating SfM models of the reef, we fabricated a mount to hold two 5 Megapixel Flir Blackfly GigE 50S5C cameras encased in waterproof enclosures on the outer sides of the pontoons, sitting just beneath the water surface. A stereo camera system grants the vehicle a larger field of view of the seafloor which permits it to cover more space in fewer passes. The max throughput we achieved from the cameras was 2Hz. Image saving was very computationally expensive and our limited processing power was a main bottleneck of the effectiveness of our system. We saved images to an onboard solid state drive through multi-threading and dedicated one processor per camera. Since the GPS is not mounted above the cameras, custom software was written which combines the GPS data and orientation of the robot (measured by the IMU) to calculate the relative pose transformation of the cameras and estimate the true location of the cameras; ensuring that each individual image was tagged with its own GPS location.

To achieve a highly accurate position estimate for both navigation and embedding location information into the images, we chose to use an RTK GPS, specifically the Emlid Reach RS2. A single RS2 GPS sensor has a position accuracy of += 2.5m, but when receiving corrective measurements from a static base station on shore, the sensor can accurately estimate its location with centimeter accuracy. The high accuracy of the RTK GPS benefits both our navigation script, ensuring image overlap, as well as the SfM model, decreasing computation time as well as giving accurate GPS coordinates of the measured data. Before surveying, we would setup the base station on shore where it would have line of sight to our survey location. The RS2 has a communication range of 8km between stations.

In addition to surveying the complexity of the reef, members of our team were interested in gathering water quality measurements. A Eureka Manta+ sensor is mounted in the rear and measures water temperature, pH, conductivity, and turbidity, all GPS tagged with the robots current location.

Missions are planned prior to deployment using the open source UAV software ardupilot [19]. From the planned geofence, a series of way points are created that follow a simple lawnmower pattern and are uploaded to the robot. Spacing between rows is determined by water depth, desired image overlap, and camera field of view. Survey areas were typically 50m by 50m and the robot could survey three different areas before depleting its two batteries.

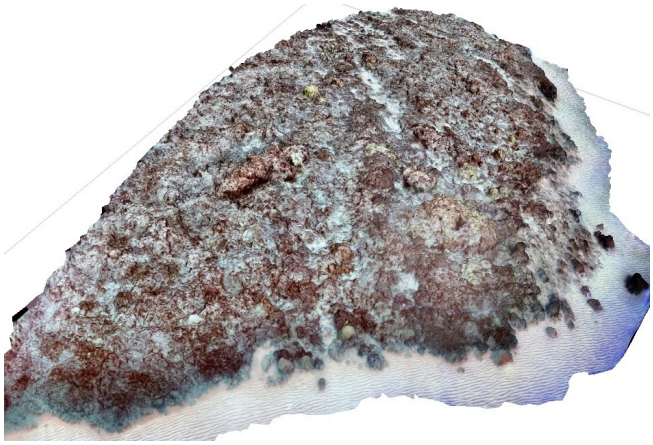

Fig. 3. A 3D reconstruction of an approximately 60m x 40m section of the fringing reef off the southern coast of Molokai, Hawaii in Nov. 2021 (Survey Site 1).

Custom hardware to interface between the cameras, GPS, water quality sensor, IMU and base computer of the vehicle is enclosed in a water tight case mounted on the top of the vehicle. Figure 2 shows the labeled vehicle components. Custom software was also necessary to integrate all the sensors, including an interface for navigating to way points with a PID controller and a differential drive kinematic motion model, as well as a live image viewer and trajectory plotter of the vehicle.

B. Field Trials in Molokai, HI

In November 2021, we deployed this platform off the southern coast of Molokai, Hawaii. The reef is under attack from terrestrial sediment deposited from the overgrazed mountain side; the terrestrial sediment impedes the reef's ability to photosynthesize, slowly suffocating it. We surveyed five sites in different regions of the fringing reef, as well as several sites in the local fish ponds [20] where only water quality measurements were recorded due to the murky water. Reef inspection missions took approximately 1 hour of run time, covering approximately 2,500 square meters and taking about 10,000 images per mission. The water depth at these survey sites ranged from three to ten meters deep. Figure 4 shows the location of each of the test sites with their reconstructed DEM.

C. Image Reconstruction

SfM relies upon finding hundreds of unique features per image that can be found in another image to calculate tie points and image correspondence. This can be difficult with underwater imagery due to the lack of light in the water column and every image being a dark shade of blue. When we first began creating the models from Hawaii, we were unable to reconstruct any of the missions due to the software struggling to find image tie points. To overcome this issue we pre-processed the images by independently

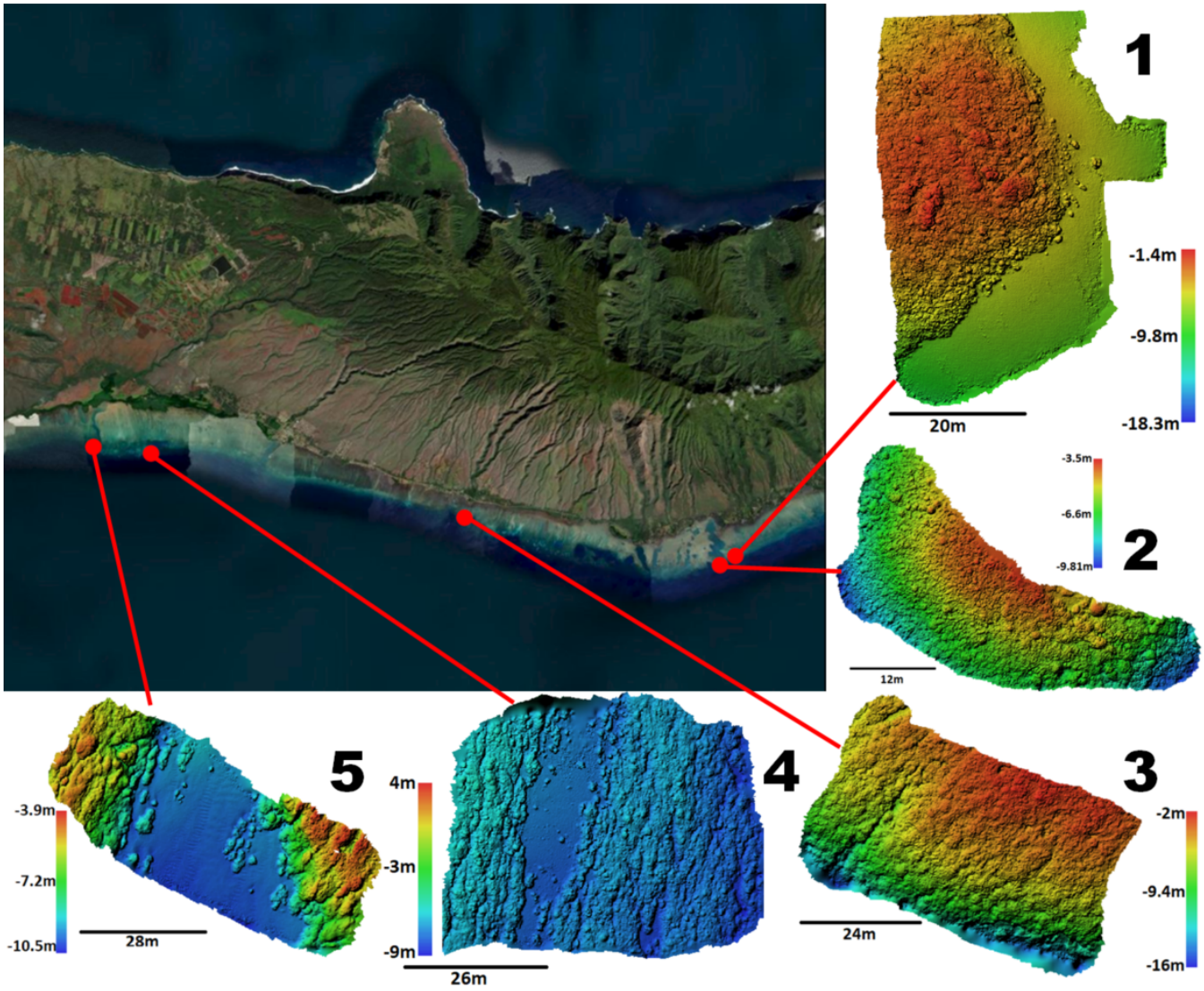

Fig. 4. Reconstructions performed off the southern shore of Molokai, Hawaii recorded in November, 2021. Labeled are the five test sites with their respective digital elevation models.

applying histogram equalization to each color channel [21]. By equalizing the color channels, the image reconstruction algorithm was able to better detect features, find tie points and associate images where it struggled before. We used Agisoft Metashape with mild depth filtering to perform 3D reconstructions of the reef. Despite only using 5 Megapixel cameras, we were able to achieve reconstructions with pixel sizes as small as 3.7mm x 3.7mm.

One of the surveyed models is shown in Figure 3. For reference, all five sites are shown in Figure 4 as DEMs. Figure 5 demonstrates the difference between simulated chain measurements and surface complexity measurements performed on the 3D model of the reef.

IV. Analysis and Evaluation of Chain Rugosity and Surface Complexity

Due to the tedious and time consuming nature of estimating a reef's rugosity with a chain, only a handful of measurements can be obtained and used to infer the complexity of the reef. Using our virtual model of the reef, we attempt to estimate the measurement error of the chain and surface complexity methods as well as show that surface complexity, a metric that can only be obtained from a 3D model by comparing the 3D surface area to the 2D area, is a more robust measurement. Figure 5 shows a visual comparison between the two methods.

A. Rotation and Translation Based Measurement Error

The first two experiments performed were designed to show that translation and rotation error in the placement of a chain can affect the recorded measurement. When out on the open water, measurement location selection is somewhat arbitrary. Researchers attempt to lay chains perpendicular to shore in an area that they deem good enough or interesting. Already these measurements face a bias by the recorder who may choose more complex environments; additionally, trying to place a chain perpendicular to shore is also subjective

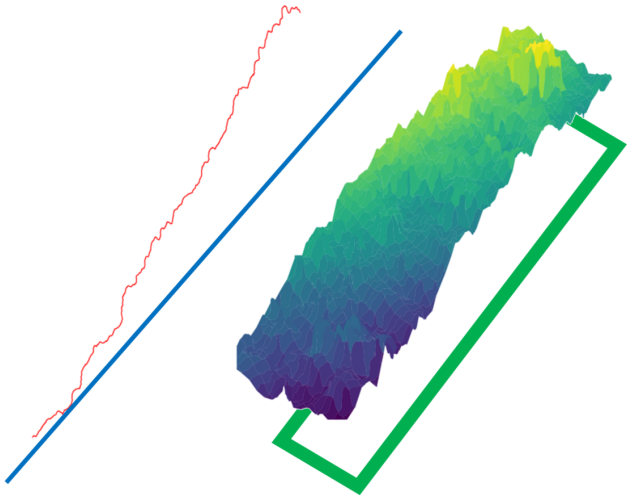

Fig. 5. A comparison of the simulated chain rugosity (left) and surface complexity (right) measurements. The chain measurement computes the ratio between the 1D distance traveled by the chain and the actual chain length. Surface complexity computes the ratio between the 3D surface area of the reef over a region and the 2D area of that region.

to bias. Translation errors may occur after a site has been selected, either when the divers go to the surface floor or the chain is dropped from the surface, there is no guarantee the chain will be in the intended spot once on the ocean floor.

The first experiment estimates the translation error that can occur when placing a chain and how much a subtle shift in location can affect the measured result. Across the five digital elevation models generated from our Hawaii data set, at each site we randomly chose a test location with a length and width equal to the length of the chain, typically 15m. We then measured twenty virtual chains that were equally spaced across the test site, a 0.75m offset, and took the mean and standard deviation of the measurements. We also calculated the relative standard deviation which is the standard deviation divided by the mean, multiplied by 100. This process was repeated 1000 times at each of the five test sites. We compared these results using the relative standard error because a surface complexity measurement can not be directly compared with a linear rugosity measurement.

The second experiment calculates the rotation error of chain measurements, following a similar process as the first experiment. Twenty chains were placed, equally rotated about the midpoint by a three degree increment. The chains were placed in a range of -30 to +30 degrees perpendicular towards shore.

To compare the accuracy of the chain rugosity measurement with the SfM surface complexity, we repeated the two experiments using surface complexity measurements instead of simulated chain measurements. A larger survey site will more accurately represent the reef, but we wanted to be able to compare surface complexity measurements with the previous chain experiments on the same scale. To accomplish this, we chose a reconstruction size that can be accomplished by a diver or an AUV taking pictures in a transect and creating a SfM model of the area.

In simulation this was done by generating a parallelogram with a set length and width that covers a randomly selected area of the model. The lengths of the area were the same as the chain lengths at each site, and 1m wide. From the DEM the parallelogram created a mask of the 2D area. The 3D surface area was calculated by triangulating the corners of each cell to create a mesh and summing up the area across the masked site. The surface complexity was then calculated by dividing the 3D area measurements by the 2D area measurements. To avoid overlap, each surface complexity measurement is separated by its width, 1m, spaced across a 15 square meter area. The rotation experiment with surface complexity measurements were still rotated around a midpoint. Due to the nature of surface complexity measurements, more overlap occurs at the midpoint leading to a smaller rotational error.

Figure 6 shows the four experiments run on data from test site 2. Figure 6(a), and 6(b), show the results of translation and rotation errors of chain rugosity measurements within the area. It can be seen that translation and rotation errors affect chain rugosity measurements by 5% and 4% respectively at test site 2. Over the same test site, the 1m wide surface complexity measurements of the same length as the chains outperformed the chain measurements with a translation and rotation error of 3% and 2% respectively. It should be noted that in certain scenarios the relative error of the chain method can exceed 10%, whereas the surface complexity metric is less susceptible to such high errors.

B. Measurements Needed to Characterize a Site

In an attempt to evaluate the number of chain measurements needed to accurately characterize the complexity of an area of the reef, we performed an experiment by grouping together measurements. The experiment initially begins with one simulated chain, measuring and recording the simulated rugosity at a random location within a test site one thousand times. The process is repeated, incrementing to two randomly placed simulated chains across the test site and averaging those measurements. This process continued until twenty random measurements were simulated with their mean recorded per iteration. For each number of chain measurements, 1000 iterations were simulated, each of the same length of chain with the same perpendicular orientation towards shore.

The experiment was repeated with surface complexity measurements to evaluate how an increased number of these measurements affect the estimated complexity of the reef. Due to the increased computation time of calculating surface complexity compared to linear rugosity, only 500 experiments were run per measurement per site, compared to the 1000 experiments run per measurement per site as used in the rugosity experiments.

As expected, the variance declines as more measurements are averaged. As seen in Figure 8, the variability of a single measurement is large, but decreases as more measurements are calculated. We expected the variability of surface complexity measurements to decrease more drastically than the

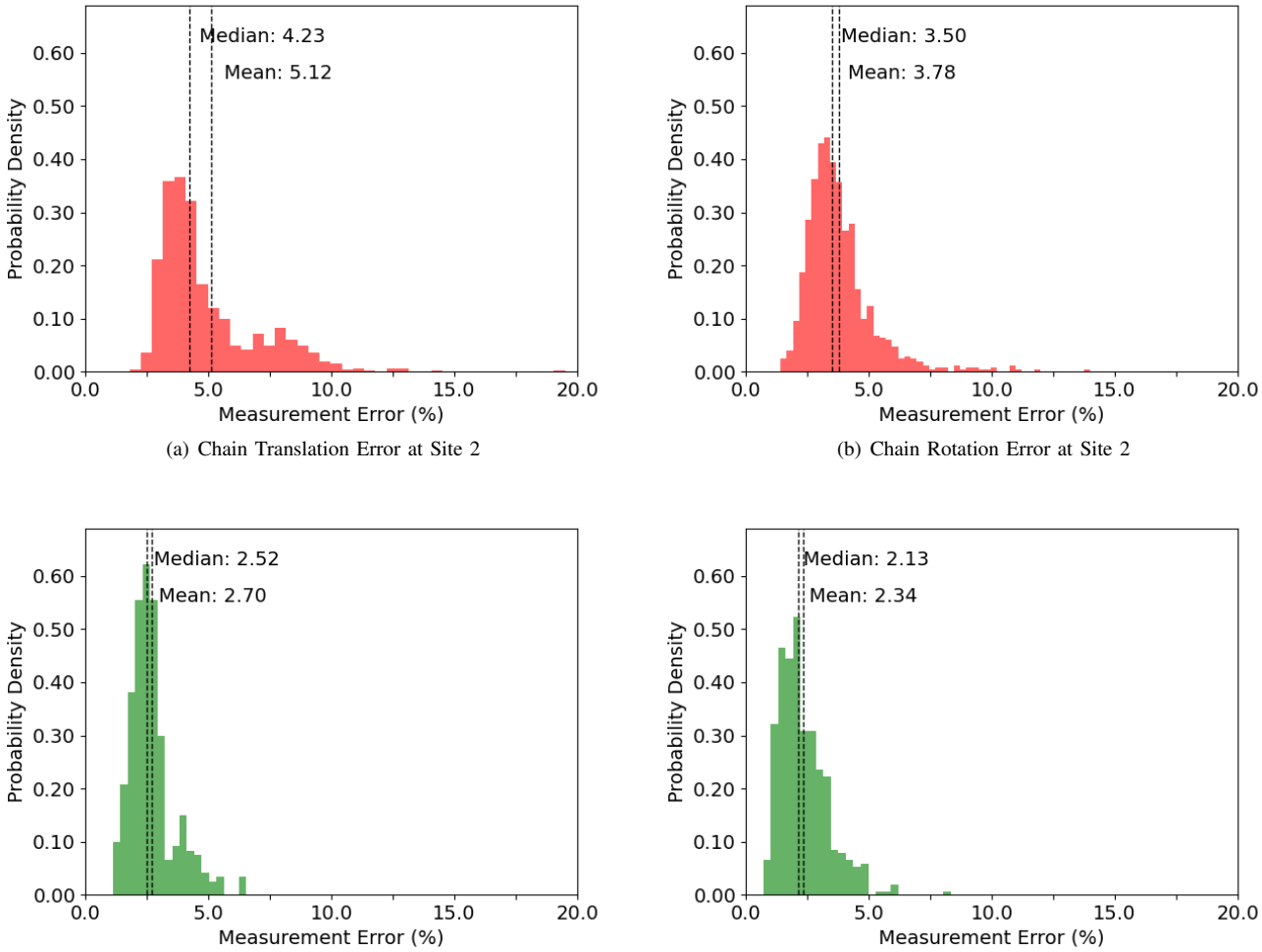

(a) Chain Translation Error at Site 2

(b) Chain Rotation Error at Site 2

(c) Surface Complexity Translation Error at Site 2

(d) Surface Complexity Error Rotation at Site 2

Fig. 6. A comparison of chain rugosity and surface complexity translation and rotation errors across site 2.

linear chain method, but both models decreased at relatively the same rate. However the more area covered, the less variance can be expected from a measurement. To further explore this we repeated the surface complexity tests but varied the widths of the area measured to be 2, 4 and 8 meters respectively. That data is shown in Figure 8. Regardless of width, measurement variance has diminishing returns on more testing with both measurements tending to not increase in accuracy after ten measurements. Measuring ten or more random sites within a 50m x 50m area in the field is unreasonable, other options would be to simply survey a larger area than a 1m wide, 15m long section of the reef, like what we accomplished with our ASV. As shown, as measurements cover a larger area, measurement variance decreases, so instead of measuring ten random one meter wide test sites, the same could be accomplished by measuring a single eight meter wide test site, or two, four meter wide test sites.

C. Evaluation of Disparity Around Sand Channels

While analyzing the different test sites, we found a scenario when in randomly testing different areas the chain method might outperform the surface complexity measurements. Test sites 4 and 5 as shown in Figure 4 both have a sand channel bisecting the reef, whereas test sites 1, 2 and 3 are one continuous piece of the reef with edges only along the outside. By randomly selecting test spots, surface complexity and chain measurements were simulated in these flat sand channels where rugosity and surface complexity values are near a value of 1, not complex at all. Some measurements comparing translation and rotation error would be performed where part of the measurement is on the sand, and part on the reef. As seen in the sand channel of test site 4, there are still parts of the reef not washed away by the sand, a chain measurement crossing this area can still measure as being complex if for say the chain is draped over a single coral head, whereas the surface complexity measurement still records a low complexity value closer to one. Since the idea behind our 1m wide, 15m long test

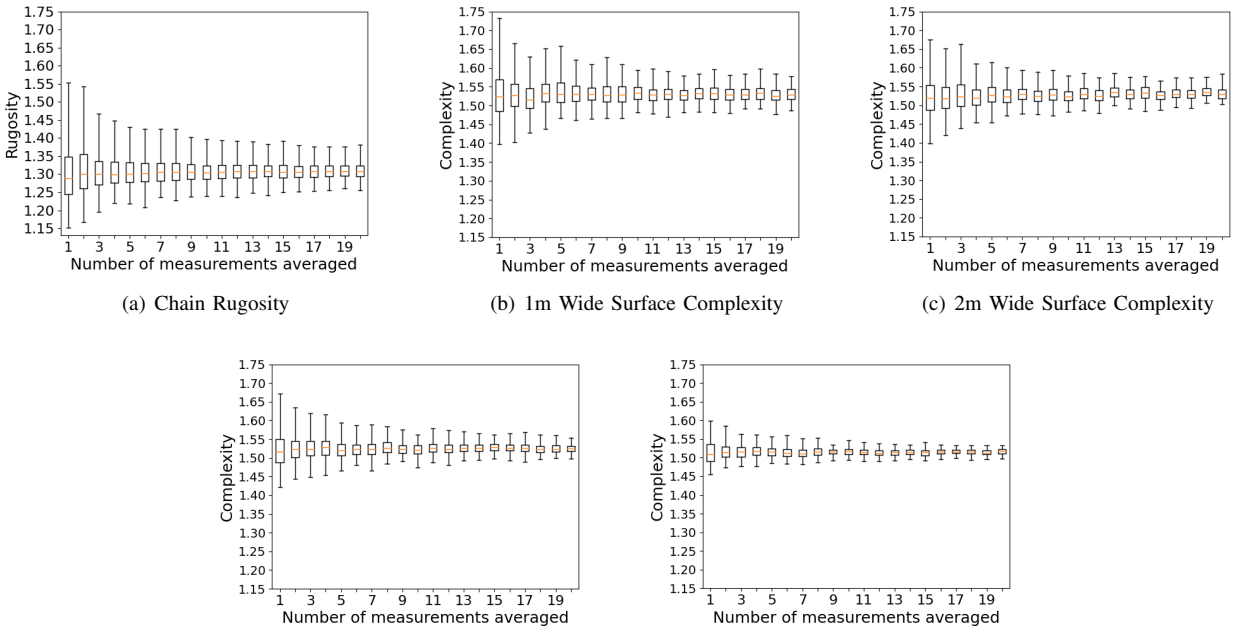

(a) Chain Rugosity (b) 1m Wide Surface Complexity (c) 2m Wide Surface Complexity

(d) 4m Wide Surface Complexity (e) 8m Wide Surface Complexity

Fig. 7. Box plots showing the variance of averaged measurements between the chain method and surface complexity of the same length with increasing widths of test measurements. As more measurements are averaged or a larger surface complexity area is measured, measurement variance between different test locations decreases.

sites was to simulate a diver recording images in a transect, we can assume a diver taking images of a reef would not take exclusive pictures of the sand and then infer the reef's complexity from those measurements. The inclusion of a sand channel would necessitate a larger survey area of the reef to understand the complexity of the reef not already overrun by sand.

Figures 8 and 9 show the combined rugosity and complexity errors between the first three sites and the latter two, demonstrating the issue with sand channels. Figure 8(a) and 8(c) show the averaged relative translation error across sites one through three, and as discussed earlier, the surface complexity measurement outperforms the chain rugosity measurement by 2.5% in terms of having a lower average variance, however, when observing the relative error of test sites four and five with sandbars, Figure 8(b) and 8(d) demonstrate that a translation error can greatly affect the measured complexity, and that in this instance the chain rugosity measurement outperforms the surface complexity measurements. Figure 9 shows the same averages but comparing rotation error instead of translation error. Rotation does not affect the data as much as translation as shown by the low error in both Figure 9(a) and 9(c), likewise, such rotations do not infer high errors even in areas over a sandbar as seen in Figures 9(b) and 9(d). Relying on the assumption that a scientist would not take exclusive measurements of a sandbar and use the low complexity value to categorize the complexity of the reef, we have found the approximate measurement error for a linear rugosity measurement via a chain to be 7.1% and 3.9% for translation and rotation as shown in Figure 8(a) and 9(a), and surface complexity measurement errors to be 4.6% and 3.4% respectively as shown in Figure 8(c) and 9(c).

V. Conclusion

In our work we have demonstrated the effectiveness of our ASV approach for reef SfM reconstruction. We've shown that the common linear chain rugosity measurement suffers from measurement error and can lead to a poor estimation of a reef's health. Through experimentation we estimated what the rotation and translation estimated error is per measurement that can be used in the field. Additionally we've shown that surface complexity measurements generated by SfM models outperform the traditional chain rugosity measurements. Future work will include upgrades for the ASV vehicle including the mounting of an echo sounder that can be used to autonomously adjust the speed and overlap requirements for the environment, as well as revamping the electronics bay with a more modular system. We are also interested in further exploring how the width of the SfM model can affect the accuracy of the inferred reef complexity, as well as how longer measurements of both SfM and chains affect accuracy. To achieve this we will likely need larger survey sites.

References

[1] M. J. Westoby, J. Brasington, N. F. Glasser, M. J. Hambrey, and J. M. Reynolds, "'Structure-from-Motion' Photogrammetry: A Low-Cost, Effective Tool for Geoscience Applications," *Geomorphology*, vol. 179, pp. 300–314, 2012.

[2] S. F. Heron, C. M. Eakin, F. Douvere, K. L. Anderson, J. C. Day, E. Geiger, O. Hoegh-Guldberg, R. Van Hooidonk, T. Hughes,

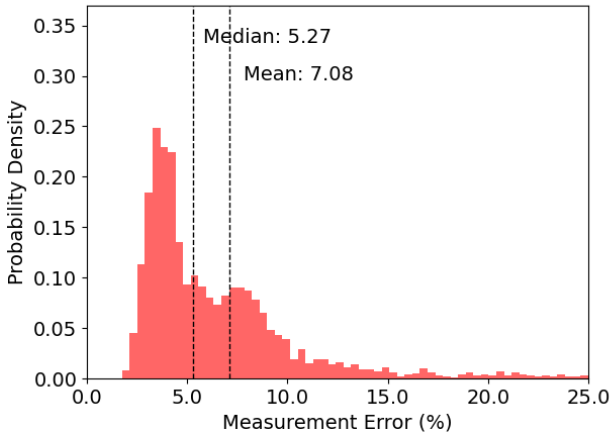

(a) Averaged Chain Translation Error across Sites 1-3

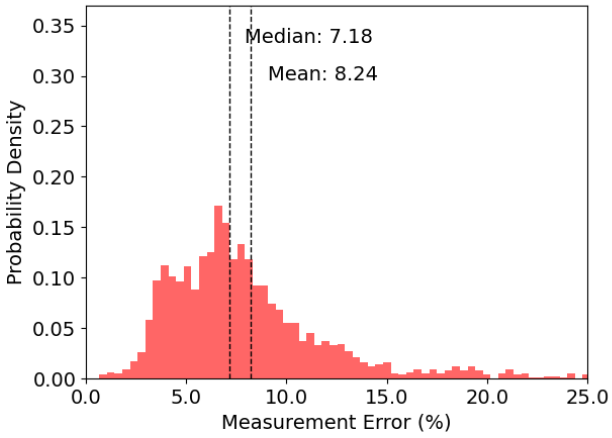

(b) Averaged Chain Translation Error across Sites 4-5

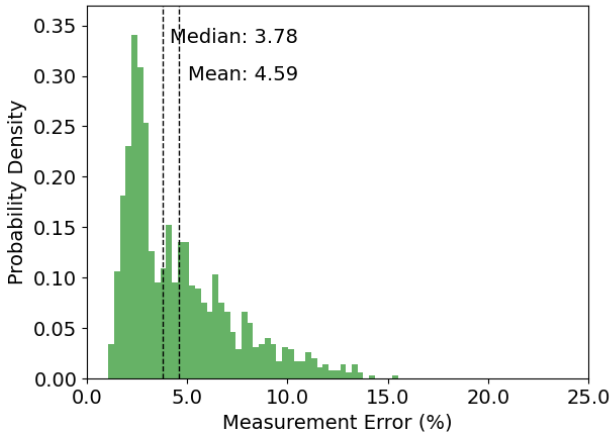

(c) Averaged Surface Complexity Translation Error across Sites 1-3

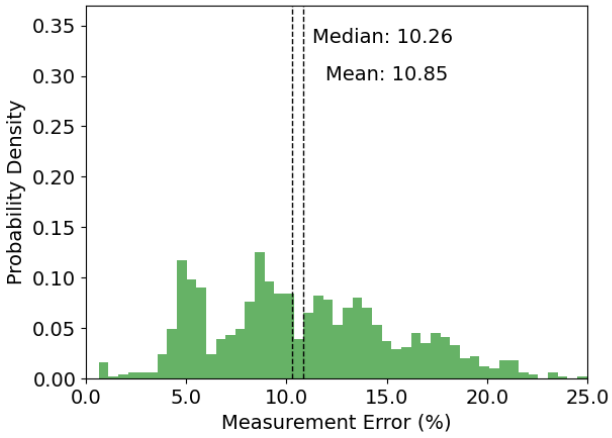

(d) Averaged Surface Complexity Translation Error across Sites 4-5

Fig. 8. Comparison of translation errors at test sites 1-3 and 4-5. The first sites do not contain a sand channel and best represent average measurement error for translation of chain and surface complexity measurements.

P. Marshall *et al.*, "Impacts of Climate Change on World Heritage Coral Reefs : A First Global Scientific Assessment," 2017.

[3] J. Burns, D. Delparte, R. Gates, and M. Takabayashi, "Integrating Structure-from-Motion Photogrammetry with Geospatial Software as a Novel Technique for Quantifying 3D Ecological Characteristics of Coral Reefs," *PeerJ*, vol. 3, p. e1077, 2015.

[4] P. Chabanet, H. Ralambondrainy, M. Amanieu, G. Faure, and R. Galzin, "Relationships Between Coral Reef Substrata and Fish," *Coral Reefs*, vol. 16, no. 2, pp. 93–102, 1997.

[5] A. M. Friedlander and J. D. Parrish, "Habitat Characteristics Affecting Fish Assemblages on a Hawaiian Coral Reef," *Journal of Experimental Marine Biology and Ecology*, vol. 224, no. 1, pp. 1–30, 1998.

[6] J. Hall, "The Risks of Scuba Diving: A Ffocus on Decompression Illness," *Hawai'i Journal of Medicine & Public Health*, vol. 73, no. 11 Suppl 2, p. 13, 2014.

[7] J. L. Schonberger and J.-M. Frahm, "Structure-From-Motion Revisited," in *Proceedings of the IEEE Conference on Computer Vision and Pattern Recognition (CVPR)*, June 2016.

[8] I. Urbina-Barreto, S. Elise, F. Guilhaumon, J. H. Bruggemann, R. Pinel, M. Kulbicki, L. Vigliola, G. Mou-Tham, V. Mahamadaly, M. Facon, S. Bureau, C. Peignon, E. Dutrieux, R. Garnier, L. Penin, and M. Adjeroud, "Underwater Photogrammetry Reveals New Links Between Coral Reefscape Traits and Fishes that Ensure Key Functions," *Ecosphere*, vol. 13, no. 2, Feb 2022.

[9] D. T. Bayley, A. O. Mogg, H. Koldewey, and A. Purvis, "Capturing Complexity: Field-Testing the Use of 'Structure From Motion' Derived Virtual Models to Replicate Standard Measures of Reef Physical Structure," *PeerJ*, vol. 7, p. e6540, 2019.

[10] T. N. F. Roach, S. Yadav, C. Caruso, J. Dilworth, C. M. Foley, J. R. Hancock, J. Huckeba, A. S. Huffmyer, K. Hughes, V. A. Kahkejian, E. M. P. Madin, S. B. Matsuda, M. McWilliam, S. Miller, E. P. Santoro, M. R. de Souza, D. Torres-Pullizaa, C. Drury, and J. S. Madin, "A Field Primer for Monitoring Benthic Ecosystems using Structure-from-Motion Photogrammetry," *Jove-Journal of Visualized Experiments*, no. 170, Apr 2021.

[11] A. Friedman, O. Pizarro, S. B. Williams, and M. Johnson-Roberson, "Multi-scale Measures of Rugosity, Slope and Aspect from Benthic Stereo Image Reconstructions," *PloS One*, vol. 7, no. 12, p. e50440, 2012.

[12] Z. Yang, X. Yu, S. Dedman, M. Rosso, J. Zhu, J. Yang, Y. Xia, Y. Tian, G. Zhang, and J. Wang, "UAV Remote Sensing Applications in Marine Monitoring: Knowledge Visualization and Review," *Science of the Total Environment*, vol. 838, no. 1, Sep 10 2022.

[13] E. Casella, A. Collin, D. Harris, S. Ferse, S. Bejarano, V. Parravicini, J. L. Hench, and A. Rovere, "Mapping Coral Reefs Using Consumer-Grade Drones and Structure from Motion photogrammetry techniques," *Coral Reefs*, vol. 36, no. 1, pp. 269–275, 2017.

[14] G. T. Raber and S. R. Schill, "Reef Rover: A Low-Cost Small Autonomous Unmanned Surface Vehicle (USV) for Mapping and Monitoring Coral Reefs," *Drones*, vol. 3, no. 2, 2019.

[15] G. Grisetti, R. Kümmerle, C. Stachniss, and W. Burgard, "A tutorial on graph-based SLAM," *IEEE Intelligent Transportation Systems*

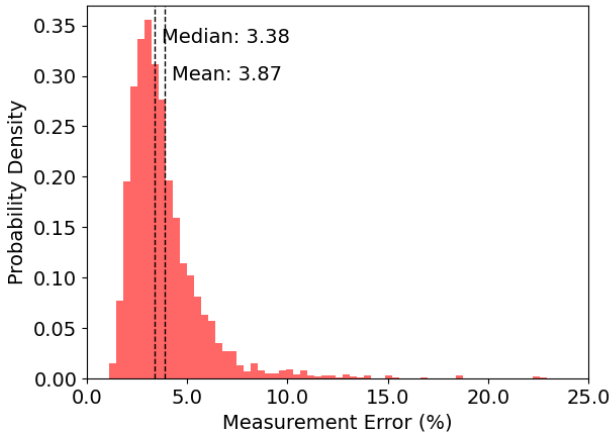

(a) Averaged Chain Rotation Error across Sites 1-3

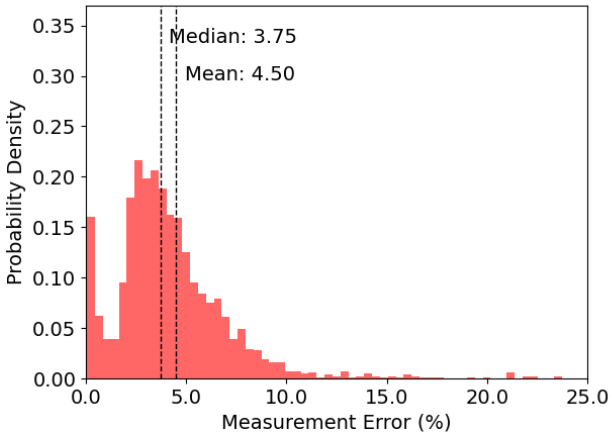

(b) Averaged Chain Rotation Error across Sites 4-5

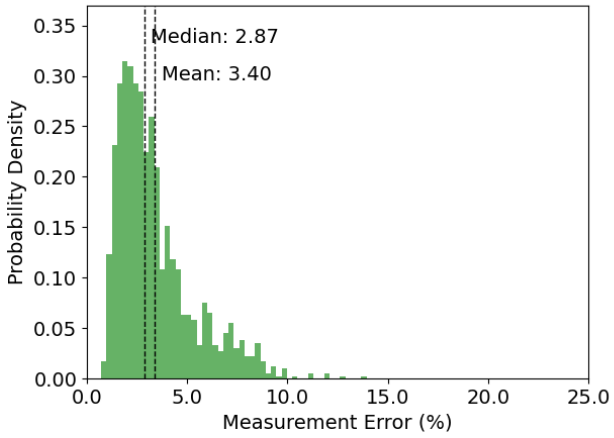

(c) Averaged Surface Complexity Rotation Error across Sites 1-3

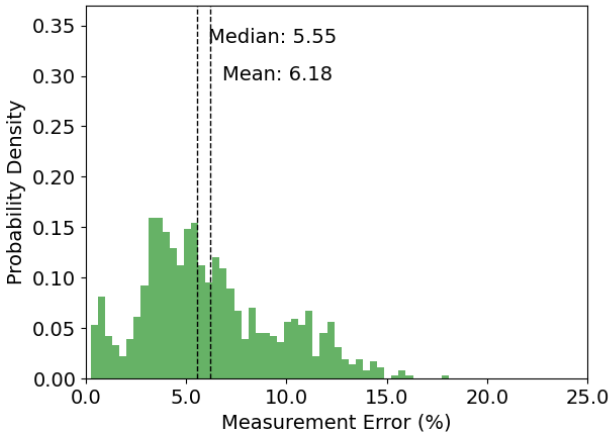

(d) Averaged Surface Complexity Rotation Error across Sites 4-5

Fig. 9. Comparison of rotation errors at test sites 1-3 and 4-5. The first sites do not contain a sand channel and best represent average measurement error for rotation of chain and surface complexity measurements.

Magazine, vol. 2, no. 4, pp. 31–43, 2010.

[16] T. Taketomi, H. Uchiyama, and S. Ikeda, "Visual SLAM algorithms: A survey from 2010 to 2016," *IPSJ Transactions on Computer Vision and Applications*, vol. 9, no. 1, pp. 1–11, 2017.

[17] D. Ribas, P. Ridao, J. Neira, and J. D. Tardos, "SLAM using an imaging sonar for partially structured underwater environments," in *2006 IEEE/RSJ International Conference on Intelligent Robots and Systems*. IEEE, 2006, pp. 5040–5045.

[18] Stanford Artificial Intelligence Laboratory et al., "Robotic Operating System." [Online]. Available: https://www.ros.org

[19] ArduPilot, "Ardupilot." [Online]. Available: https://ardupilot.org/

[20] B. A. Costa-Pierce, "Aquaculture in Ancient Hawaii," *BioScience*, vol. 37, no. 5, pp. 320–331, 1987.

[21] A. Forrest, "Colour Histogram Equalisation of Multichannel Images," *IEE Proceedings-Vision, Image and Signal Processing*, vol. 152, no. 6, pp. 677–686, 2005.